

Numerical Study on the Asymmetry in Wake Steering of Wind Turbine under Yawed Conditions

Dezhi Wei¹, Nina Wang², Decheng Wan^{1}, Sergei Strijhak³*

¹ Computational Marine Hydrodynamics Lab (CMHL), School of Naval Architecture, Ocean and Civil Engineering, Shanghai Jiao Tong University, Shanghai, China

² Key Laboratory of Far-shore Wind Power Technology of Zhejiang Province, Huadong Engineering Corporation Limited, Hangzhou, China

³ Ivannikov Institute for System Programming of the Russian Academy of Sciences, Moscow, Russia

*Corresponding author

ABSTRACT

Wake redirection via active yaw control is a promising strategy to improve the whole wind farm performance. To successfully apply such an operational control in the real-world engineering, it is necessary to have a precise knowledge of the yawed turbines and their wakes. In the current work, a series of numerical simulations are performed by the high-fidelity SOWFA tool, to study the occurring asymmetry in oppositely signed yaw angles, as well as its effects on wake-steering performance. The simulation results demonstrate that the wake curl is asymmetric between positive and negative yaw angles, arising from the interaction of the counter-rotating vortices with the vertical wind veer. Some key wake properties are also observed to be asymmetric with respect to the yaw angle direction, especially the lateral wake deflection, which can affect the efficiency of active yaw control. What's more, a load study of wake steering is conducted, showing that the positive yaw offsets are less harmful to the tested NREL 5MW wind turbine. In conclude, this work emphasizes the necessity and importance of considering the yaw direction in implementing yaw-based wind farm control.

KEY WORDS: Opposite yaw directions; Asymmetry in wake steering; Wake flow property; Structure load

INTRODUCTION

Wind energy is a kind of renewable energy with great development prospects (Chehouri et al, 2015). In order to maximize wind energy extraction within the limited available land, multiple turbines are commonly installed in an organized array in the wind farm. However, a consequent drawback is the strong wake interference among turbines, which has a significant impact on the wind farm performance, not only increasing turbine loads, but also decreasing energy capture. To mitigate the negative effects of wake interaction, many efforts have been made before. For instance, some scholars paid attention on altering wind farm layout, example studies include (Park et al, 2015;

Kirchner-Bossi et al, 2018), and increasing streamwise distance between the consecutive turbines was suggested. What's more, some active wake control strategies were proposed, which can be divided into two classes, one about reducing the axial induction of the upstream turbine (Annoni et al, 2016), and the other is the wake redirection techniques, including pitch angle control, tilt angle adjustment and active yaw control (Bastankhah et al, 2019; Miao et al, 2017). In Fleming et al. (2014), they tested several wake redirection strategies and found that active yaw control is the most promising method to improve wind plant performance. It is implemented by intentionally misaligning the upstream turbine rotor to the incoming wind direction, thereby deflecting the wake and avoiding the downstream wind turbines. Although the power output of the yawed turbine itself is reduced, the total power of entire wind farm can potentially increase, as the downwind turbine is less affected by the upstream wakes.

To better apply active yaw control in practice, a detailed knowledge of the yawed turbine wake and its interaction with downstream turbines is required. Howland et al. (2016) conducted a wind tunnel measurement to study the yawed wake morphology under uniform inflow. They observed a curled wake shape and attributed its formation to a pair of counter-rotating vortices shed from the top and bottom of the rotor plane. Apart from deforming the wake, Fleming et al. (2018) further highlighted other roles of the counter-rotating vortex pair (hereafter, CVP), which were found to deflect the wake of an aligned downstream turbine, even if it was non-yawed. This is called "secondary wake steering" phenomenon, and is proven to be critical for the wake evolution of turbine array under yawed conditions. Additionally, also a number of studies focused on the possibilities of power optimization through intentional yaw misalignment. For instance, Campagnolo et al. (2016) experimentally studied the performance of three turbine rows, and they observed that, for the case where the wind turbines were in the flow 4 rotor diameters apart, the total wind farm power production can increase about 4% by using a closed-loop wake deflection controller. A numerical simulation of Gebraad et al. (2016) on six wind turbines also demonstrated the capability of active yaw control. In their works, a 13% increase of the combined power under yawed conditions was seen compared to the baseline non-yawed case.

The asymmetry of wake steering in the opposite yaw directions is also an important topic in the wind energy community. Vollmer et al. (2016) studied the yawed wake characteristics under different atmospheric thermal stabilities, and found the significant effect of the ambient wind on turbine wake evolution. In the stable boundary layer, a high degree of asymmetry in wake deflection was shown with respect to the yaw direction. Focusing on the wake flow behind a single yawed turbine, Bastankhah et al. (2015) did lots of wind tunnel tests in different conditions. By comparing the mean wake contour in the vertical cross section, they observed a clear asymmetry between the positive and negative yaw angles, particularly in the wake shape and the location of maximum velocity deficit. Furthermore, Bartl et al. (2018) found that the asymmetry of wake flow was more pronounced under the lower inflow turbulence level. Besides the wake behavior, the asymmetry in wake steering is also reflected in the power gain. For instance, in Fleming et al. (2015), two aligned turbines spaced by 7 rotor diameters were studied under different first turbine yaw angles. The results revealed a positive effect of yaw angle control, and pointed out the asymmetric distribution of total power enhancement. Miao et al. (2017) reported similar phenomenon, they reported that, after deducting the power losses caused by yaw, an increase in the combined power was only measured when the upstream turbine was yawed positively. In order to better utilize yaw misalignment for improving wind farm control, the above studies are far from enough, especially in the asymmetry of wake steering that the current work is concerned about, a more comprehensive and in-depth investigation is required. For example, the quantitative analysis on some key wake properties and the discussion of structural loads with respect to yaw direction are left open until now. For this purpose, we conducted numerous large eddy simulations for one-turbine and two-turbine scenarios under different yaw angles. We also hope to provide some new insights on how to reflect the asymmetry of wake steering in the empirical engineering wake models.

NUMERICAL METHODS

Description of SOWFA

In this work, a CFD-based analysis is performed to explore the asymmetry in wake steering. The simulations are conducted by SOWFA, which is a high-fidelity wind plant modeling tool. Extensive details on the SOWFA tool are collected by Churchfield et al. (2012), in here, only a brief introduction is given.

The large eddy simulation (LES) technique is adopted in SOWFA, which directly solves the large-eddy scale dynamics, and the contribution of the sub-grid scales to the resolved flow field is parameterized by the eddy-viscosity model. What's more, in the lower boundary, both the viscous and SGS effects need to be considered, however, directly resolving the large scales near the lower surface is computationally expensive as the mesh must be fine enough. To avoid the restriction, Moeng model is applied to specify the lower surface-boundary condition, which is a common practice in the atmospheric LES community. Furthermore, the actuator line model (2002) is introduced to parameterize the turbine-induced forces for computational efficiency.

Simulation Setup

Each of the SOWFA simulation can be divided into two stages, referred to as the "precursor" simulation and "successor" simulation, respectively.

(1) "precursor" simulation.

The simulation is firstly performed on a domain with laterally periodic boundaries, to generate a realistic turbulent atmospheric boundary layer (hereafter, ABL). In particular, as shown in Fig 1, the computational

domain in the current work spans 3000 m in both the x- and y-coordinate directions and 1000 m in the z- coordinate direction, and it is discretized uniformly into $300 \times 300 \times 100$ grid points. The initial potential temperature profile was taken to be 300 K from the ground up to 700 m, and in the next 100 m upwards, it increased linearly to 308 K; above 800 m, the rise rate was set to 0.003 K/m. The surface temperature flux and the surface roughness height were taken to be 0 K/m and 0.001 m, respectively, typical of neutral stability and offshore conditions. To avoid the 'stuck' phenomenon, the horizontally mean wind speed at the hub height was not aligned with the x- direction of domain (270°), but came from southwest (240°). In a whole, the numerical setting is the same as that in Ref (Churchfield et al, 2012), which has been validated before and represents a realistic scenario. We first ran the precursor simulation for 18000 s, to ensure that the ABL flow reached a quasi-equilibrium state; then, we ran it for another 1000 s, and during that time, the instantaneous turbulent data on the upwind boundary planes were saved at every time step, which would be used as the inflow boundary conditions for the "successor" simulation. (2) "successor" simulation.

In the second stage, the wind turbine was added into the developed flow field, and lot of simulations were conducted for a single turbine and two-turbine scenarios under different yaw angles. Specifically, the wind turbine used is the NREL 5MW baseline turbine, it has a rotor diameter of 126 m and a hub height of 90 m. Note that, the computational domain and background mesh were inherited from the precursor simulation, but the boundary conditions were different. As aforementioned, the upstream boundary condition was specified by the saved turbulent data, and the downstream boundaries were no longer periodic but outflow, allowing the turbine-induced wake to exit without cycling back. What's more, in order to better capture the turbine wake structures, we locally refined the mesh around the wind turbine, as indicated by the black solid rectangular region in Fig 1. Corresponding to the computational time of the precursor simulation, all test cases in the second stage ran for 1000 s, and the time step was taken to be 0.02 s, to ensure that the advancing of blade tip was less than one grid cell per time step. Over the simulation, data of the power output and structural loads were extracted but only in the last 600 s, for the purpose of eliminating transient effects.

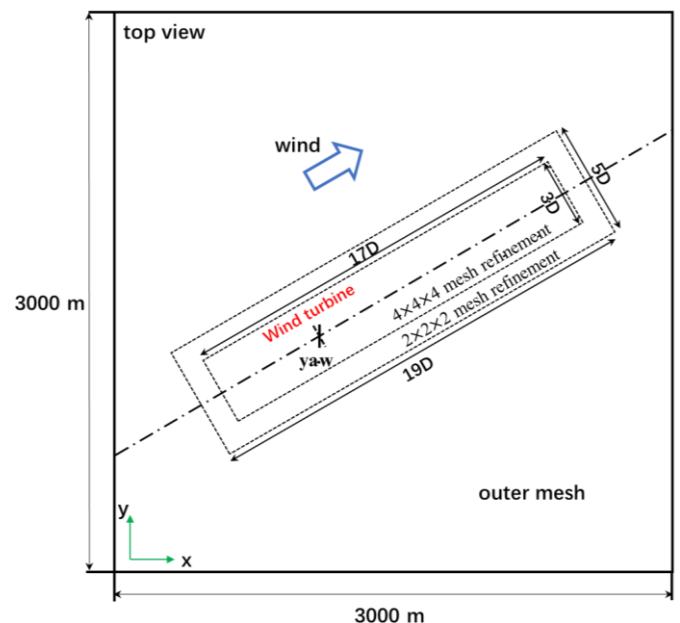


Fig.1 Schematic view of the computational domain and mesh resolution

RESULTS

Inflow characteristics

The main characteristics of the simulated boundary layer flow are displayed in Fig 2. It can be seen that, the horizontally averaged streamwise velocity is not uniform in the vertical direction, showing strong wind shear, and the mean wind speed is about 8 m/s at the hub height. What's more, as a result of the Coriolis force, the wind direction changes with height. For the particular case considered here, the change in wind direction across the rotor disk is around 2° . Although the value is small, it is likely to affect the turbine wake development. As apparent in Fig 2(c), the inflow turbulence intensity decreases with increasing height, which is in good agreement with real conditions, and the hub height turbulence level is around 6%.

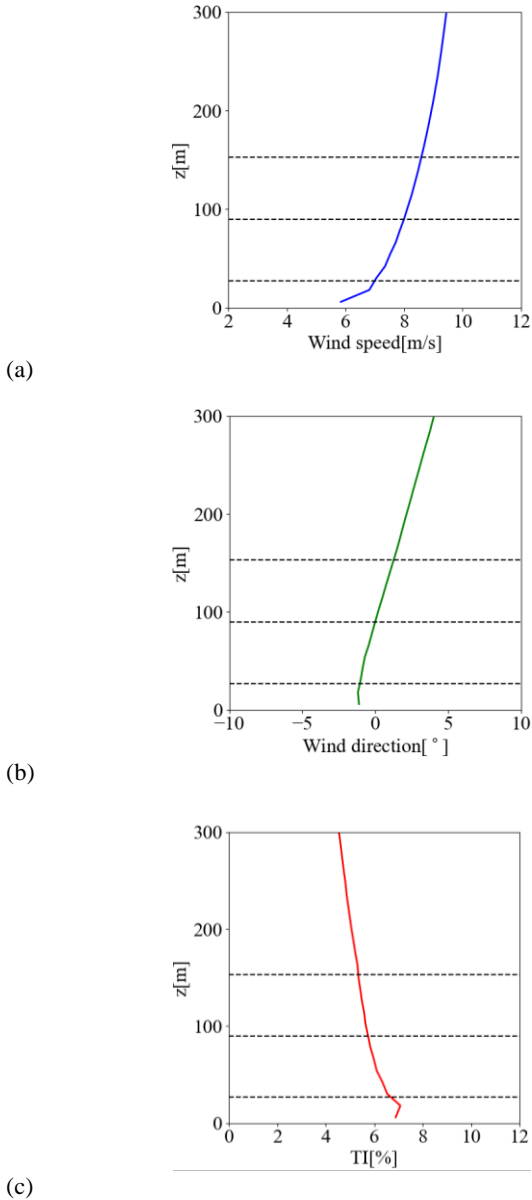


Fig.2 Vertical profiles of (a) horizontally averaged wind speed, (b) wind direction, and (c) turbulence intensity of the inflow. The horizontal dashed lines represent the top-tip, hub, and bottom-tip heights.

One-turbine scenario

We first study a single wind turbine under different yaw angles (0° , $+30^\circ$ and -30°). Note that, in the current work, the positive yaw angle is defined as a clockwise turning of the rotor when seen from above. Fig. 3 shows the vertical contour plots of the mean velocity deficit at different downstream distance, i.e., the changes of wind speed in turbine wake field with respect to the background flow. It is shown that, unlike an approximately elliptical wake profile for the non-yawed wind turbine, a turbine in yawed conditions has a kidney-shaped cross section. And as going downstream, the yawed wake becomes more complicated. For instance, in the case of $\gamma = +30^\circ$, the lower right part of the wake even detaches from the whole wake structure at the downwind location of $x/D = 10$.

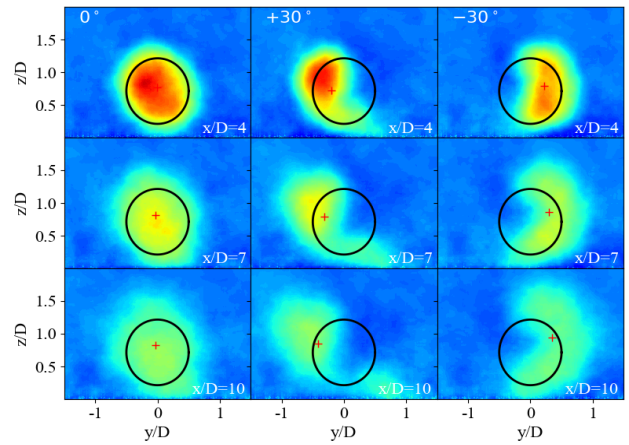


Fig.3 Contour plots of the normalized velocity deficit in the vertical planes at $x/D = 4, 7$, and 10 downwind of the turbine. The black circle denotes the wind turbine position.

In order to provide a more quantitative description of the mean turbine wake for different yaw angles, we parametrize the velocity contour in the vertical cross section and simplify it into a two-dimensional line. The detailed execution process is as follows:

- (1) Slice the wake contour into several points in the lateral and vertical directions;
- (2) Extract the wake center at each vertical height level by applying the method of "center of mass";
- (3) Repeat the procedure in step (2) from the bottom tip to the top tip of the rotor area;
- (4) Connect the wake centers at different heights to obtain an arch-shaped curve representing the yawed turbine wake shape.

As apparent in Fig 4, the turbine wake is slightly tilted, even for the non-yawed case. Specifically, the wake flow is shown to be asymmetric with respect to the central vertical axis and is slightly skewed towards the left. This can be explained by the Coriolis effect, which makes the incoming wind direction change with height, as shown in Fig 2(b). What's more, for the yawed turbine cases, an obvious asymmetry in wake curl between positive and negative yaw angles is noticed. In particular, the wake shows a larger deformation in the positive yaw case, especially in the lower section, while for $\gamma = -30^\circ$, a significant bulge is visible in the upper part of turbine wake. According to previous studies (Fleming et al, 2018), the asymmetry in wake shape is attributed to the interaction of the counter-rotating vortex pair with the vertical wind veer. Moreover, take a look at the intersection point of the two-dimensional lines for $\gamma = \pm 30^\circ$, as well as the intersection of the vertical centerline with the parametric line of the non-yawed wake, it can be found that, the wake tends to move upwards as proceeding downstream, regardless of the turbine operating conditions. This is

considered to be related with the non-uniform incoming flow and the presence of lower surface.

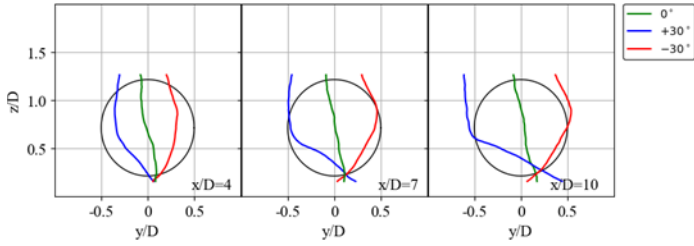


Fig.4 Parameterization of the wake shape under different yaw angles.

The wake influencing region is a main wake property, and its variation against the downwind distance has attracted wide attention among researchers. To explore the difference in the wake expansion behavior of positively vs. negatively yawed turbine, a simple method is adopted here to define the wake area, consisting of all points where the normalized velocity deficit exceeds 0.05.

The results for different yaw angles are shown in Fig 5. One can see that under the non-yawed conditions, the wake area increases with the downstream distance. What's more, compared to the baseline case, a smaller wake region is observed under yaw misalignment conditions, due to the decreased projected area of turbine rotor facing the incoming wind. More importantly, there is a fairly large difference between positive and negative yaw angles. Particularly, in the far wake region, as the wake proceeds downstream, the wake area gradually decreases for positive yaw but increases under negative yaw. This asymmetry can be attributed to the difference in wake evolution. As indicated by Fig 3, for $\gamma = -30^\circ$, the wake structure remains intact at different downwind positions. Arising from the entrainment from the surrounding air, the wake expands and affects a larger cross-sectional area. However, when going towards positive yaw offset, the turbine wake evolution becomes more complicated. As shown in Fig 3, with going downstream, the lower wake structure gradually detaches from the whole. And as a result of the high incoming turbulence level at lower altitudes, the mixing processes around the detached low-speed flow structure is strong, which contributes to a fast wake recovery, making the velocity deficit gradually lower than the specified threshold. Consequently, in the far wake region, the wake area is observed to decrease under positive yaw. This is greatly different from the assumptions of the commonly-used analytical models, in which, regardless of the yaw direction, the far wake is assumed to expand approximately linearly.

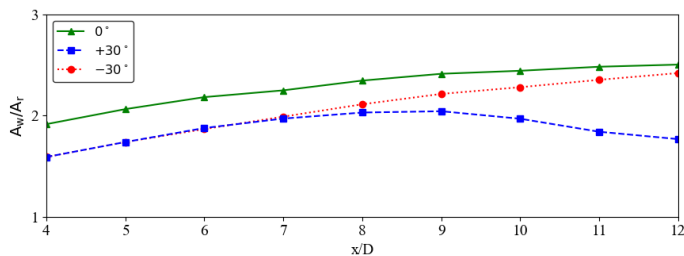


Fig.5 Variation of the normalized wake area for different yaw angles. The inflow turbulence intensity at hub height is $TI_h = 0.06$.

To get a deeper insight on the evolution of yawed wake area, we further explore the influence of incoming turbulence level and yaw angle magnitude. Fig 6 offers a summary comparison of the variation in wake area with the downstream distance under different operating conditions. The wake boundary is still defined by an isopach of 95% of the free stream velocity.

As shown in Fig 6, in the region not very far from the turbine rotor, the

wake does expand around linearly as assumed in the analytical wake model. However, further downstream, it can be seen that the wake area changes between positive and negative yaw offsets are of great different. To be specific, a decrease of wake area is detected in the far wake, and more significant at higher turbulence intensity. This is because the high inflow turbulence level enhances the mixing processes, allowing the detached wake structure to recover faster, so that the velocity deficit can reach the set wake boundary threshold within a shorter distance. Additionally, for a smaller yaw angle, the wake region is shown to only slightly decrease after $x/D=10$. The lower vorticity intensity is likely the responsible factor, which makes the position where the wake structure separates to move back. And before the separation point, the wake area is more affected by the ambient turbulence and, thus, expands with going downstream.

Under negative yaw offsets, the turbine wake in all three test cases enlarges its area with increasing downwind distance, arising from the same reason mentioned earlier, i.e., the wake structure remains intact during its evolution. What's more, increasing the turbulence level from $TI_h = 0.06$ to $TI_h = 0.10$ is seen to only have a small influence, except for a larger wake area in the higher ambient turbulence intensity.

According to the above discussion, the effects of yaw direction on the wake expansion cannot be ignored, and it also hints at the irrationality of the linear wake expansion adopted by the commonly-used analytical models. Another thing to note is that the above analysis on wake expansion is based on the numerical simulations. In future studies, the results will be further verified through wind tunnel experiments, and the variation of yawed wake area will be investigated under more operating conditions.

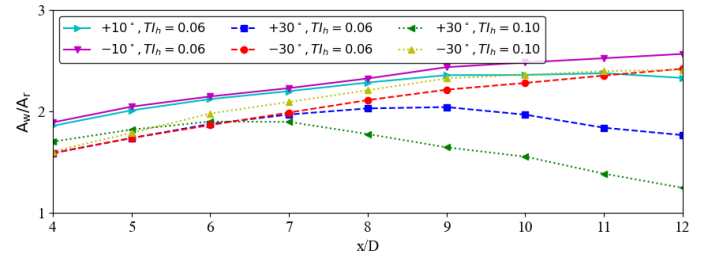


Fig.6 Variation of the normalized wake area for different yaw angles ($\gamma = 0^\circ, \pm 10^\circ, \text{ and } \pm 30^\circ$) and inflow turbulence intensity levels ($TI_h = 0.06, 0.10$).

Apart from the wake area, wake deflection is also a key wake property, as the mechanism behind active yaw control is to deflect the upstream wake away from the downwind turbines. In previous studies, several possible methods have been proposed in the literatures to define the wake center. For example, (1) take the point with the maximum velocity deficit at each downwind position; (2) apply a two-dimensional Gaussian to fit the vertical wake profile and regard the point of maximum correlation as the wake center.

However, both of the two approaches have limitations. Specifically, the first one is sensitive to the measurement uncertainty, and it is less representative of the entire wake contour. In addition, the latter one only works well for purely Gaussian profile, however, as visible in Fig 3, the wake is obviously different from Gaussian. This indicates that using the Gaussian fitting method may not obtain a satisfactory result. In order to avoid the above restrictions, a method of "center of mass" is adopted here to provide a reasonable assessment of wake center deflection. In the application, the wake area should be delineated at first, which is defined as the region where the value of velocity deficit profile is larger than 0.05. Then, we calculate the average of the coordinates for all points in the defined wake region, and the obtained result is the wake center.

Fig 7 displays the results for different yaw angles. As is shown, there is an obvious asymmetry in wake deflection between positive and negative yaw angles, and a larger deflection magnitude is observed in the positive yaw. Similar results have also been reported in previous studies. In Bartl et al (2018), the interaction of rotating wake with turbine tower is considered to be the cause of the asymmetric lateral wake trajectory, however, in the current simulations, the tower and nacelle are not modelled. Different to Bartl et al. (2018), we guess the asymmetric wake deflection may stem from the sense of turbine rotation, as it is the only source of asymmetry other than the yaw angle direction in the test cases.

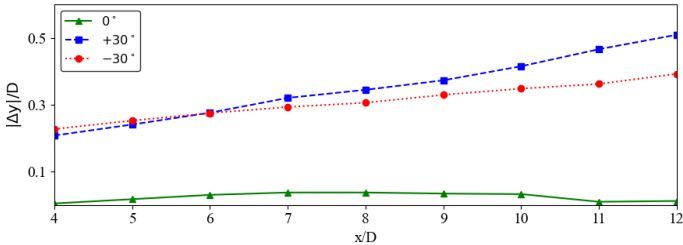


Fig.7 Variation of the normalized lateral wake deflection magnitude for different yaw angles ($\gamma=0^\circ, +30^\circ, -30^\circ$).

In addition to the lateral wake deflection, the wake center position in the vertical direction under different yaw conditions are also extracted through the method of "center of mass" and the results are depicted in Fig 8 by different symbols. One can see that, although no vertical tilt is applied to the turbine rotor, the turbine wake still deflects in the positive z direction, even for the non-yawed turbine. This is because of the non-uniform incoming wind and the presence of the lower boundary surface. To be specific, affected by the vertical wind shear, high turbulence intensity and strong kinematic stress are produced at the top-tip height behind the wind turbine, which promotes the upward wake diffusion; and at lower altitude, the ground suppresses the downward wake expansion, causing to an upward movement of the whole wake. What's more, as apparent in Fig 8, for non-zero yaw offsets, the wake center deflects upward with different magnitudes as moving downstream, and the z-displacement in the positive yaw angle is higher than that under negative yaw. The asymmetric vertical deflection may be related to the distribution of vertical velocity component in the yawed turbine wake (Wei et al, 2021).

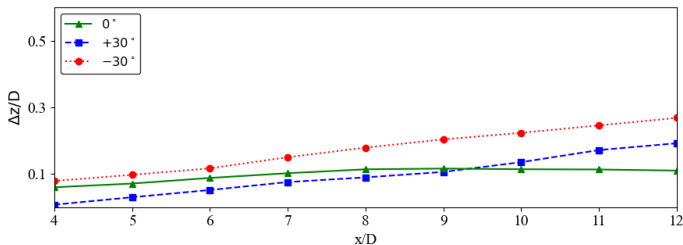


Fig.8 Variation of the normalized vertical wake deflection for different yaw angles ($\gamma=0^\circ, +30^\circ, -30^\circ$).

Two-turbine scenario

Most previous studies are concerned on the yawed wake flow characteristics and the amount of increase in wind farm efficiency achieved by active yaw control. In comparison, discussions on structural loads of turbine rotor have received less attention. However, the intentional yaw misalignment may increase unsteady loading on the yawed turbine itself and the downstream wind turbines, and further, leading to increased probability of component failure.

In this section, two wind turbines spaced by 7 rotor diameters in the streamwise direction are studied under different yaw angle distributions,

where the front turbine is yawed by $0^\circ, +30^\circ$ and -30° , and the second turbine maintains non-yawed. The case name is appended by "BSL", "+30°Yaw" and "-30°Yaw", respectively.

In our previous work (Wei et al, 2021), the total power output of the two-turbine array has been analyzed. A net gain in the overall power production was only seen with the positively-yawed front turbine, arising from the asymmetric lateral wake deflection mentioned earlier. In this section, more attention will be paid to the difference of key structure loads between positive and negative yaw.

As indicated by Schulz et al. (2017), the lift and drag forces acting on the blade airfoils is the main contributor to the turbine loads. Therefore, examining the distribution characteristics of the aerodynamic element at typical azimuths can help to explain the variations of structure loads. In this section, we first analyze the properties of angles of attack and local relative velocity around 0° and 180° azimuths under steady, sheared winds for positive and negative yaw angles, and the results are shown in Fig 9. Note that, for the sake of simplicity, no induction effect is considered here, i.e., sketches in Fig 9 are only for illustrative purposes.

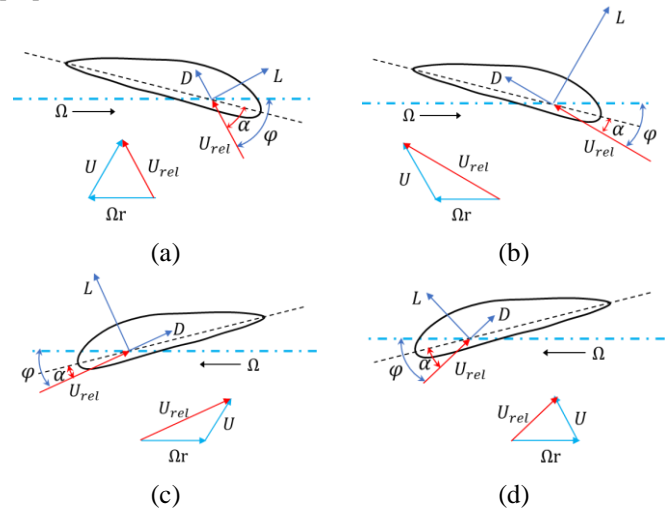


Fig.9 The asymmetric distribution of the angle of attack (α) and local relative velocity (U_{rel}) between positive and negative yaw angles. 0° azimuth corresponds to the straight upward blade orientation. (a) positive yaw angle, 0° azimuth, (b) negative yaw angle, 0° azimuth, (c) positive yaw angle, 180° azimuth, (d) negative yaw angle, 180° azimuth.

As apparent in Fig 9, there is an obvious asymmetry between the positive and negative yaw angles in blade airfoil aerodynamics. Specifically, for the positive yaw offset, a small U_{rel} and a large α are noticed at 0° azimuthal angle; while in the lower part of turbine rotor, the trigonometric relationship of the velocity components is opposite to that at 0° azimuth angle, and the inflow speed at the lower height is smaller because of the vertical wind shear, therefore, at 180° azimuth, a larger U_{rel} magnitude and a smaller α value are detected. What's more, the asymmetry about the 0° – 180° azimuth is still presented for the negative yaw angle. Of special note is that the blade airfoil at the upper rotor part has a larger relative inflow velocity and a smaller angle of attack, in comparison to the positive yaw offset; and at 180° azimuth, an almost opposite distribution to the 0° azimuthal angle is visible. Consequently, it is reasonable to suppose that, in the negative yaw, the difference in loading levels between the upper and lower half of turbine rotor is stronger.

From the above analysis, it can be concluded that the azimuthal distribution of angle of attack and relative inflow velocity at the blade airfoil are asymmetric in the oppositely signed yaw misalignments,

arising from the non-uniform shear inflow and turbine yaw. Of course, even under non-yawed conditions, the sole presence of the sheared inflow can also cause an asymmetry in the distributions of α and U_{rel} . By adding the yaw offset, one can see an increased oscillation degree for both the two quantities, i.e., the asymmetry in the azimuthal distribution is amplified, which might have profound consequences on the turbine load.

Next, three representative structure loads are studied: M_{oop} , it is defined as the bending moment acting at the blade root location, pointing to the tangential direction of the rotor rotation path. The high value of M_{oop} indicates an increased unsteady blade load at the rotor revolution frequency, which may increase the fatigue damage risk. The yaw bearing moment M_{yaw} represents the side-side imbalance of the rotor blade forces, it is aligned with the vertical axis of turbine tower and can affect the reliability of yaw drive components. Special focus is also given to the change of M_{tilt} , which describes the fore-aft bending moment about the intersect point of the low-speed shaft axis and the vertical tower axis. In order to provide a quantitative comparison of the above loads, the RMS (root-mean-square) and STD (standard deviation) values for their time histories are computed, and the results are displayed in Figs.10-12, where the RMS quantity is shown with bar charts, and the error bar indicates the standard deviation.

Fig. 10 presents the variation in M_{oop} with different yaw control actions. Take a closer look at the front turbine at first, an overall reduction in the RMS value of M_{oop} is shown for the yawed cases due to the decreased effective rotor area. Another interesting phenomenon is the large difference in loading levels under different yaw directions. In particular, with respect to the baseline case, the STD of the blade-root bending moment decreases in positive yaw but increases for negative yaw misalignment, implying its contribution to the blade fatigue damage.

Compared with the first turbine, the second turbine yields increased STD quantity in all three cases, largely due to the increased turbulence intensity and the wake meandering phenomenon. Of course, with except to the above factors, the upstream steered wake also plays a role in the yawed cases. It partially shields the second wind turbine, making its blades circulate in and out of the wake flow, and thus, causing a drastic change in M_{oop} . Additionally, arising from the reduced wind velocity in the front turbine wake, the RMS value for the second turbine is found to decrease in the baseline case.

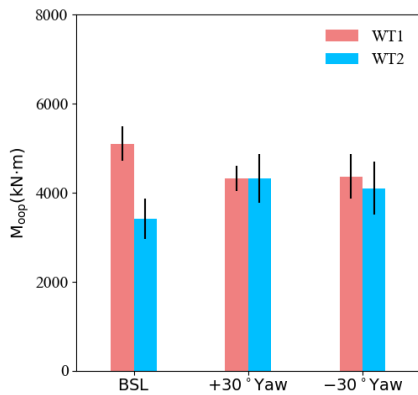


Fig.10 RMS and STD values for the time history of the blade out-of-plane bending under different yaw angle combinations.

As for the yaw bearing moment, it seems surprising at first glance since the RMS value for the first turbine in the baseline case is of the same order as that in the yawed cases, indicating a limited influence of turbine yaw. On the one hand, this is because the tested NREL 5-MW turbine has three blades, which causes an asymmetric load as there are always two blades on one side. On the other hand, the wind turbine is

operated in the atmospheric boundary layer, unbalanced aerodynamic forces imposing upon the turbine blades often occurs due to the atmospheric turbulence effects. For instance, when an instantaneous turbulent structure passes through one part of turbine rotor, the loads on the three blades are not equal. This also contributes to the yaw bearing moment.

Also apparent in Fig 11 is that, the RMS value for the downwind turbine is larger in the yawed cases, and it shows different changes against the first turbine yaw angle. The asymmetric wake deflection between positive and negative yaw angles is likely the responsible factor for the difference. Specifically, as visible in Fig 7, a larger lateral wake deflection is measured for the positive yaw offset, indicating that the downwind turbine is less affected by the upstream low-speed wake flow in such scenario, thereby decrease the lateral flow asymmetry causing a relatively small RMS quantity.

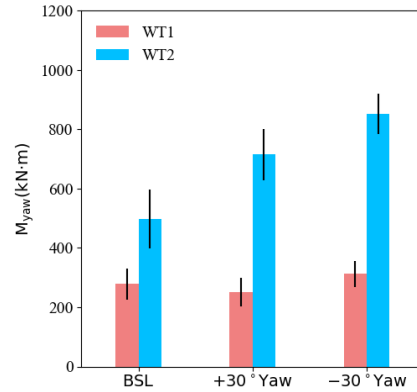


Fig.11 RMS and STD values for the time history of the yaw bearing moment under different yaw angle combinations.

At last, the tilting moment of wind turbine is examined. As can be seen in Fig 12, when the first turbine yawed +30°, the RMS value of this load is reduced, while a distinctive increase is shown for the negative yaw, demonstrating a significant impact of yaw direction on the tilting moment. The reason for such asymmetry is deemed to be related with the difference in blade loading levels between the upper and lower half of turbine rotor mentioned in Fig 9.

Additionally, compared to the baseline case, a larger increase in the RMS value of M_{tilt} is found for the second turbine operating in the wake of a negatively-yawed upstream turbine. This can be explained by the "added yaw angle" attached to the downwind turbine. In particular, as described by Fleming et al. (2018), the transverse velocity in upstream yawed wake changes the local wind direction perceived by the non-yawed downwind turbine, making it actually have a yaw angle in the same direction as the upstream turbine, so M_{tilt} behaves similarly.

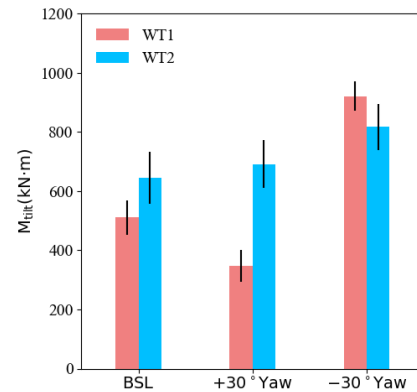


Fig.12 RMS and STD values for the time history of the tilting moment under different yaw angle combinations.

CONCLUSIONS

Special focus in the present work is given to the asymmetry of wake steering in oppositely signed yaw angles, which is an interesting phenomenon in active yaw control. To have a precise knowledge of the asymmetric wake behavior between positive and negative yaw offsets, as well as its influence on the downstream wind turbine, large-eddy simulations were performed for one-turbine and two-turbine scenarios under different yaw conditions.

Firstly, take a look at the wake evolution behind a single turbine with opposite yaw misalignments. Arising from the interaction of counter-rotating vortex pair with vertical wind veer, an obvious asymmetry in wake curl between positive and negative yaw angles was noticed. What's more, we also made some quantitative analysis on the changing of some key wake properties with downstream distance. For positive yaw, the wake area defined by an isopach of 95% of free stream velocity was found to decrease in the far wake region, and the effect got stronger in higher ambient turbulence intensity. This is an important finding of the current work, which violates the linear wake expansion assumption adopted by the commonly-used analytical models. However, the assumption shows good applicability to negative yaw offsets, i.e., the turbine wake enlarges its area as moving downstream. Moreover, the lateral wake center deflection was also studied, which was shown not to be symmetric with respect to the yaw direction, and a larger deflection magnitude was measured for the positive yaw. This result may stem from the sense of turbine rotation, as it is the only source of asymmetry other than the yaw direction.

Secondly, we paid attention to the structural loads of the yawed turbine. An obvious asymmetry in blade airfoil aerodynamics was observed between the positive and negative yaw angles, owing to the non-uniform sheared inflow and the difference in the trigonometric contribution of airfoil angular velocity to relative wind speed. And compared to the positive yaw angle, a stronger difference in the loading levels between the upper and lower half of rotor plane was found under the negative yaw offset. Accordingly, a higher RMS value of the tilting moment and an elevated STD quantity of the blade-root bending moment were detected for the negative yaw. However, the yaw bearing moment was an except, it was shown to be less affected by the turbine yaw, and was mainly driven by the atmospheric turbulence structure and the "spontaneous yaw moment". From the above analysis, the positive yaw offset is less harmful in loads to the wind turbine, and it has been demonstrated to enhance the overall wind farm power production in previous studies. Consequently, for the considered NREL 5-MW turbine, as well as other similar types of wind turbines, mainly positive yaw is recommended for wake steering in the north hemisphere.

ACKNOWLEDGEMENTS

This work was supported by the National Natural Science Foundation of China (51879159, 52131102), and the National Key Research and Development Program of China (2019YFB1704200), to which the authors are most grateful.

REFERENCES

Annoni, J, Gebraad, P, Scholbrock, A, Fleming, P, van Wingerden, JW (2016). "Analysis of axial-induction-based wind plant control using an engineering and a high-order wind plant model," *Wind Energy*, 19, 1135–1150.

Bartl, J, Mühle, F, Schottler, J, Sætran, L, Peinke, J, Adaramola, M,

Hölling, M (2018) "Wind tunnel experiments on wind turbine wakes in yaw: effects of inflow turbulence and shear," *Wind Energ. Sci.*, 3, 329–343.

Bastankhah, M, Porté-Agel, F (2015). "A wind-tunnel investigation of wind-turbine wakes in yawed conditions," *Journal of Physics: Conference Series*, 625(1).

Bastankhah, M, Porté-Agel, F (2019). "Wind farm power optimization via yaw angle control: A wind tunnel study", *Journal of Renewable and Sustainable Energy*, 11, 023301.

Campagnolo, F, Petrovic, V, Schreiber, J, Nanos, EM, Croce, A, Bottasso, CL (2018). "Wind tunnel testing of a closed-loop wake deflection controller for wind farm power maximization," *Journal of Physics: Conference Series*, 753, 032006.

Chehourri, A, Younes, R, Ilincă, A, Perron, J (2015). "Review of performance optimization techniques applied to wind turbines," *Applied Energy*, 142, 361–88.

Churchfield, M, Lee, S, Michalakes, J, Moriarty, P (2012). "A numerical study of the effects of atmospheric and wake turbulence on wind turbine dynamics," *Journal of Turbulence*, 13, N14.

Fleming P, Gebraad, P, Lee, S, van-Wingerden, JW., Johnson, K, Churchfield, M, et al (2014). "Evaluating techniques for redirecting turbine wakes using SOWFA," *Renewable Energy*, 70, 211–218.

Fleming, P, Gebraad, P, Lee, S, van-Wingerden, JW, Johnson, K, Churchfield, M, et al (2015), "Simulation comparison of wake mitigation control strategies for a two-turbine case," *Wind Energy*, 18, 2135–2143.

Fleming, P, Annoni J, Churchfield M, Martinez L, Gruchalla KM, Lawson MJ (2018). "A simulation study demonstrating the importance of large-scale trailing vortices in wake steering," *Wind Energy Sci.*, 3, 243–255.

Gebraad, P, Teeuwisse, F, van-Wingerden, JW, Fleming, P, Ruben, S, Marden, JR (2016). "Wind plant power optimization through yaw control using a parametric model for wake effects-a CFD simulation study," *Wind Energy*, 19, 95–114.

Howland, MF, Bossuyt, J, Meyers, MT, Meneveau, C (2016) "Wake structure in actuator disk models of wind turbines in yaw under uniform inflow conditions," *J. Renewable Sustainable Energy* 8, 043301.

Kirchner-Bossi, N, Porté-Agel, F (2018). "Realistic wind farm layout optimization through genetic algorithms using a Gaussian wake model," *Energies*, 11,3268.

Miao, W, Li, C, Pavesi, G, Yang, J, Xie, X (2017). "Investigation of wake characteristics of a yawed HAWT and its impacts on the inline downstream wind turbine using unsteady CFD," *Journal of Wind Engineering and Industrial Aerodynamics*, 168: 60–71.

Park, J, Law, KH (2015). "Layout optimization for maximizing wind farm power production using sequential convex programming," *Applied Energy*, 151, 320–34.

Schulz, C, Letzgus, P, Lutz, T, Krämer, E (2017). "CFD study on the impact of yawed inflow on loads, power and near wake of a generic wind turbine," *Wind Energy* 20:253–268.

Sørensen, JN., Shen, WZ (2002). "Numerical modeling of wind turbine wakes," *Journal of fluids engineering*, 124(2): 393-399.

Vollmer, L, Steinfeld, G, Heinemann, D, Kühn, M (2016). "Estimating the wake deflection downstream of a wind turbine in different atmospheric stabilities: an LES study," *Wind Energ. Sci.*, 1, 129–141.

Wei, DZ, Wan, DC, Hu, CH (2021). "Numerical Simulations of Asymmetrical Wake Flows of a Yawed Wind Turbine," *Proceedings of the Thirty-first (2021) International Ocean and Polar Engineering Conference Rhodes, Greece, June 20–25, 2021*, PP. 429-435.